Jacobs Publishers

OPEN ACCESS

Jacobs Journal of Inorganic Chemistry

Original Article

Effect of some group-II metals on RDX

Lemi Türker[*1]

Middle East Technical University Department of Chemistry, Ankara-Turkey

*Corresponding author: Lemi Türker, Middle East Technical University Department of Chemistry, Ankara-Turkey,- Fax: +90-312 2103200; E-mail: lturker@metu.edu.tr

Received Date: 10-03-2018

Accepted Date: 12-28-2018

Published Date: 01-07-2019

Abstract

The effects of Be, Mg and Ca atoms on the well-known explosive material, RDX are considered within the constraints of density functional theory at the levels of B3LYP/6-31++G(d,p) and ω B97X-D/6-31++G(d,p). Various structural, quantum chemical properties and IR spectra of the composite systems, RDX + metal are obtained and discussed. Although, Be and Mg do not affect RDX molecule appreciably, Ca atom causes the cleavage of one of the N-NO_2 bonds and rupture of the RDX ring system. The RDX+Mg composite has the most narrow inter frontier molecular orbital energy gap among the composites considered. In all the cases, the metal atom acquires some positive charge.

Key words: RDX; Cyclonite; Hexogen; Beryllium; Magnesium; Calcium; Density functional theory

Introduction

RDX (Cyclonite, hexogen, cyclotrimethylene trinitramine or 1,3,5-trinitrohexahydro-*sym*-triazine, $C_3H_6N_6O_6$) an important modern molecular explosive, has attracted the attention of scientists for many years since it has been synthesized by Henning in 1899 for medicinal use and used as an explosive in 1920 by Hertz [1,2].

RDX is mainly obtained in the industry by direct nitrolysis process (Woolwich) in which hexamethylene tetramine is directly treated with a large excess of strong HNO_3 [1,3-5] at a temperature of 20-25 ˚C. On the other hand, in the Bachman (Combination Process) process, which is also an industrial process for RDX, the reaction mixture contains HNO_3, NH_4NO_3, acetic anhydride and acetic acid in addition to hexamine [1,3,5].

The most stable crystalline structure of RDX belongs to α–RDX. It is one of the most effective energetic materials with applications ranging from explosives and propellants [6]. The measured impact sensitivity (h_{50}) value of RDX is 28 cm, comparable to the value of 32 cm for HMX (octahydro–1,3,5,7–tetranitro–1,3,5,7–tetrazocine) which is one of the high-performance energetic materials with various applications [6,7].

The experimental crystal density (ρ) of RDX has been found to be 1.81 g/cm^3 and its detonation performance has been reported as 8.75 km/s for velocity of detonation (D) and 34.70 GPa for detonation pressure (P) in the literature [4,5,7-10]. RDX is a widely used, high-brisance explosive. It is very stable, relatively insensitive (as compared to PETN (penta erythrioltetra nitrate) [10].

On the other hand, there exist some experimental and theoretical studies on RDX-metal interactions. Density functional theory study of interactions of cyclotrimethylene trinitramine (RDX) with metal-organic framework was reported [11].

A mathematical flow model is described for one-dimensional detonations in mixtures of high explosives with small inert metal particles. The model and observed detonation velocities for mixtures of RDX and Cu are used to calibrate the assumed equation of state constant as a function of the particle mass fraction [12]. Methods to investigate the igniter/propellant interaction were reported. The tests were performed with black powder and some RDX/metal mixtures including copper [13].

De Paz and Ciller [14] used Stewart's new semi–empirical method MNDO–PM3 (PM3) for the calculation of gas phase heat of formation of RDX. The heat of formation ($\Delta H^{o}_{f\ (PM3)}$) value was reported as 40.44 kcal/mol in the study. Catoire et al. [15] presented the thermochemical properties of RDX by means of the Density Functional Theory (DFT) along with a protocol developed for energetic compounds. They obtained $\Delta H^{o}_{f\ (RDX)}$ as 44.4 kcal/mol.

On the other hand, certain metals usually are added into explosive compositions to improve their performances. Aluminum and magnesium are the most widely used materials for this purpose. Titanium, zirconium and tungsten are also used [16]. In the present study, the interaction of Be, Mg and Ca metals with RDX molecule are investigated within the limitations of density functional theory (DFT).

Method of calculation

Geometry optimizations of all the structures leading to energy minima were initially achieved by using MM2 method followed by semi-empirical PM3 self-consistent fields molecular orbital (SCF MO) method [17,18] at the restricted level [19,20]. Subsequent optimizations were achieved at Hartree-Fock level using various basis sets hierarchically. Then, geometry optimizations were managed within the framework of density functional theory [21,22], finally at the level of RB3LYP /6-31++G(d,p) [19] and ωB97X-D/6-31++G(d,p) [23,24]. The exchange term of B3LYP consists of hybrid Hartree–Fock and local spin density (LSD) exchange functions with Becke's gradient correlation to LSD exchange [22,25]. Note that the correlation term of B3LYP consists of the Vosko, Wilk, Nusair (VWN3) local correlation functional [26] and Lee, Yang, Parr (LYP) correlation correction functional [27]. Note that ωB97XD functional provides excellent geometries and energies. It has high HF percentage (the second as a long-range corrected functional), which helps mitigate the self-interaction error and the difficult excitation energies required for charge transfer reactions [23,24].

The vibrational analyses were also done. The total electronic energies are corrected for the zero-point vibrational energy (ZPE). The stationary points to energy minima were proved in all the cases by calculation of the second derivatives of energy with respect to the atom coordinates. The normal mode analysis for each structure yielded no imaginary frequencies for the 3 *N*–6 vibrational degrees of freedom, where *N* is the number of atoms in the system. This indicates that the structure of each molecule corresponds to at least a local minimum on the potential energy surface. All these calculations were done by using the Spartan 06 package program [28].

Results and discussion

Several chemicals are added to energetic materials to produce heat, light, smoke, noise and motion. However, not all the chemicals are compatible for every energetic material. Some of them are inert towards a particular energetic material but some of them are not. In the present study, interactions of some alkaline earth (group-II) metals, namely Be, Mg, and Ca on RDX are considered at the molecular level.

Structures

The metals considered presently are characterized with full either 2 s, 3 s or 4 s outermost orbitals. Their first ionization potentials are 9.28 eV, 7.61eV and 6.09 eV, respectively for Be, Mg and Ca having electronegativity values of 1.5, 1.2 and 1.0 [29].

Figure 1 shows the optimized structures of the metal composites (1:1 molecule:atom) of RDX. The calculations have been done by using two different functionals within the constraints of DFT and the same basis set. The figure also depicts the direction of the dipole moments. Both types of the calculations yield similar optimized structures. The ring is in the chair conformer form and the NO_2 groups occupy axial positions. Note that although Be and Mg do

not cause any drastic changes on RDX structure, Ca atom results in cleavage of one of the nitramine (N-NO_2) bonds and also dramatically affects one of the C-N bonds of the ring to rupture. The broken C-N bond (ca. 3.50 Å) yields an open structure (see Figure 2). The figure shows the bond lengths and/or distances where the cleaved N-NO_2 linkage was 4.45 Å and 4.29 Å , respectively for the first (RB3LYP /6-31++G(d,p), method-I) and the second (ω B97X-D/6-31++G(d,p), method-II) type calculations. The C-H bonds (not shown in the figures) remain intact. The broken C-N bond (ca.3.50 Å) yields an open structure. The Mg atom slightly affects one of the N-O bonds without any cleavage. Also note that in the Be composite, all the NO_2 groups are in axial positions whereas in the Mg composite two of them are in the axial and the third one occupies the equatorial position.

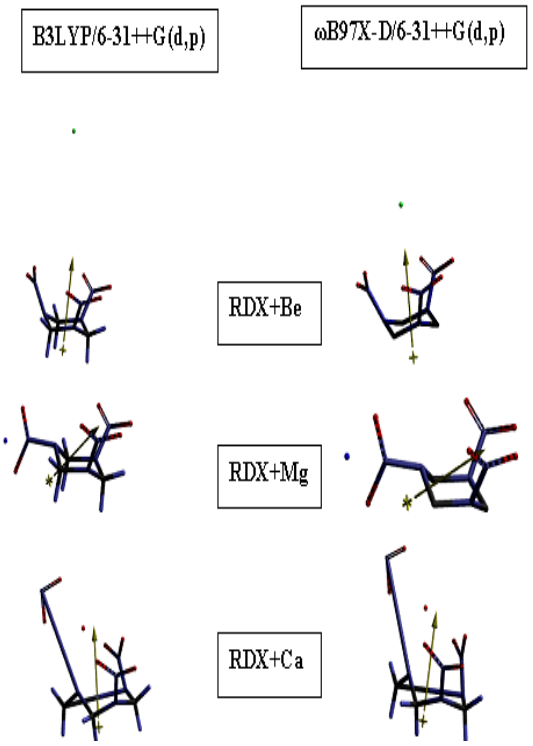

Figure 1: Optimized structures of the composite systems considered.

Inspection of **(Figure2)** reveals that B3LYP/6-31++G(d,p) level of calculations generally estimate bond lengths/distances slightly more than the ωB97X-D/6-31++G(d,p) level.

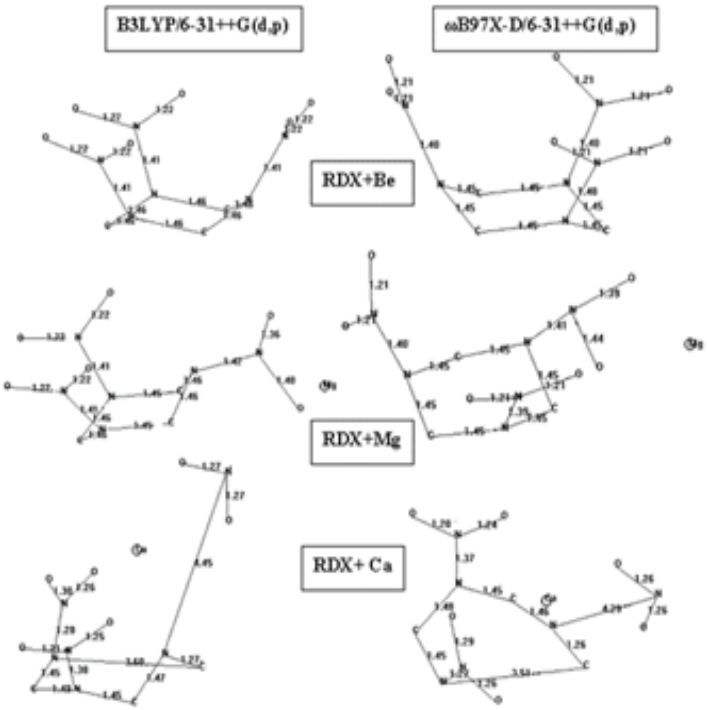

Figure 2: Bond lengths (Å) of the composites considered (hydrogens and Be not shown).

(Figure 3) shows the electrostatic charges (ESP) on the atoms in electrostatic units. Note that the ESP charges are obtained by the program based on a numerical method that generates charges that reproduce the electrostatic potential field from the entire wavefunction [28].The figure indicates that the metal atom gets some positive charge. The order is Be<Mg<Ca which is inversely in accord with the electronegativity values of those metals (1.5, 1.2 and 1.0 for Be, Mg and Ca, respectively [29]). In the case of RDX+Ca composite the expelled NO2 moiety possesses a negative overall charge (-0.73 and -0.74 by method-I and II-, respectively) which indicates that expelled NO2 group is in the form of pre-nitrite.

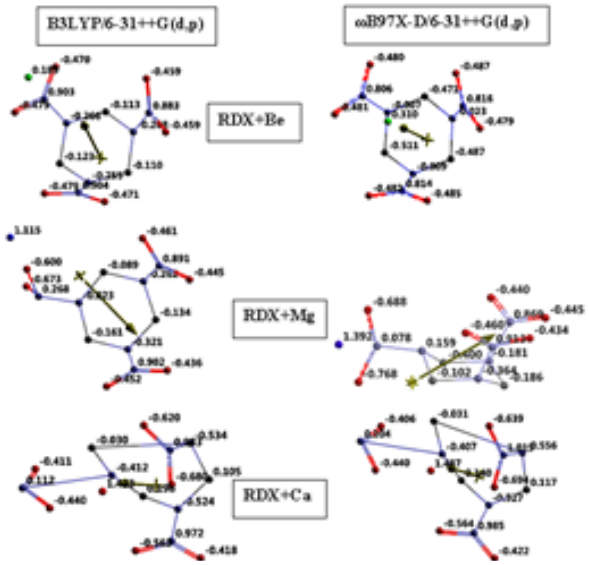

Figure 3: Electrostatic charges (ESP) on atoms of the composite systems considered (hydrogens not shown).

(Figures 4 and 5) stands for the IR spectra of the composites obtained by methods I and II, respectively. The peaks at about 1669 cm-1 in Figure 4 and 1733 cm-1 in (**Figure 5**) stand for asymmetric stretching of N-O bonds of axial NO2 groups which are coupled with N-NO2 bending modes. The peaks about 1300-1360 cm-1 are due to symmetrical N-O stretchings and N-NO2 vibrations (in the case of Be composite). Various ring vibrations occur at 900-1000 cm-1. In the case of Mg composite, the peaks about 700 cm-1 in (**Figure 4**) and 740 cm-1 in (**Figure 5**) stand for N-NO2 stretchings coupled with N-O stretchings and ring vibrations. As for the RDX+Ca case, the peaks about 1623 cm-1 in Figure 4 and 1690 in **(Figure 5)** are due to asymmetrical N-O stretchings and N-NO2 bendings (coupled with each other) of only one of the remaining NO_2 groups of the decomposed composite. Similar vibrations for the other NO2 group occurs at 1470-1510 cm^{-1} in **(Figure 4**) and 1548 cm-1 in **(Figure 5).** The group of bands in the region of 1280-1340 cm^{-1} **(Figure 4)** and 1340-1412 cm^{-1} **(Figure 5)** stand for symmetrical stretchings of N-O and N-NO_2 coupled with some ring vibrations. The peak at 1259 cm-1 in Figure 4 and 1335 in **(Figure 5)** are asymmetrical stretchings of the expelled NO2 group.

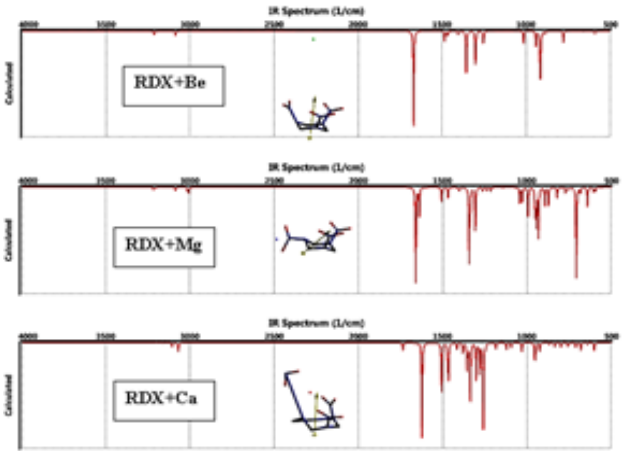

Figure 4: IR spectra of the composites considered (B3LYP/6-31++G(d,p)).

Table 1. Various properties of the composites considered.

	B3LYP/6-31++G(d,p)			ω B97X-D/6-31++G(d,p)		
Composite	**Dipole moment**	**Polarizability**	**Ovality**	**Dipole moment**	**Polarizability**	**Ovality**
RDX+Be	7.64	54.41	1.44	7.48	53.37	1.44
RDX+Mg	10.67	54.81	1.39	13.12	53.86	1.38
RDX+Ca	7.40	55.61	1.46	6.73	54.49	1.43
Dipole moments in Debye. All belong to C1 point group.						

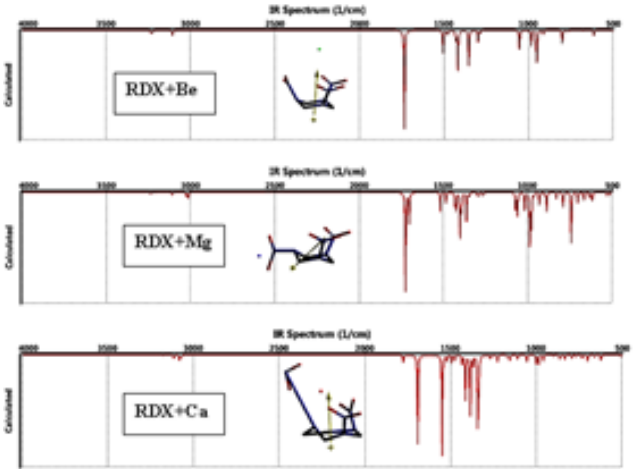

Figure 5: IR spectra of the composites considered (ω B97X-D/6-31++G(d,p)).

(Table 2) shows the total electronic energy (E), zero-point vibrational energy (ZPE) and the corrected total electronic energy (E_c) values of RDX (in the same conformer form as in the composite structures) and the composite systems considered. The energies in the table stand for energetically stable forms but in the case of RDX+Ca composite RDX skeleton has been decomposed by the effect of calcium atom.

(Figures 6 and 7) show the distribution of some of the molecular orbital energies of the composite systems by the calculation methods of I and II, respectively.

The RDX+Be case is characterized with the large HOMO-LUMO (the frontier molecular orbital energy gap, Δε) and the HOMO-NHOMO gaps. The abbreviation NHOMO stands for next HOMO. The RDX+Ca case also has large HOMO-LUMO gap however it is a decomposed system. The relatively narrow frontier molecular orbital (FMO) energy gap of RDX+Mg case could be due to some sort of electrostatic interaction between the positively charged metal atom and negatively charged oxygen atom of the NO_2 group. As seen in **(Figure 2),** that N-O bond next to the Mg atom is somewhat elongated getting closer to Mg atom. Another point to be mentioned about the RDX+Mg case is that the inner-lying molecular orbital energies are highly closely spaced exhibiting a dense distribution.

As for the methods applied, ω B97X-D/6-31++G(d,p) level of calculations predict lower HOMO but higher LUMO energies and larger FMO gaps as compared to the predictions of B3LYP/6-31++G(d,p) level (Table 3). The HOMO energy order is RDX<RDX+Ca<RDX+Mg<RDX+Be and RDX-

Table 2: Various energies of RDX and the composites considered

Table 2. Various energies of RDX and the composites considered.						
	B3LYP/6-31++G(d,p)			**ω B97X-D/6-31++G(d,p)**		
System	**E**	**ZPE**	**E_c**	**E**	**ZPE**	**E_c**
RDX	-2356267.23	373.51	-2355893.72	-2355538.72	382.38	-2355156.34
RDX+Be	-2394785.71	374.00	-2394411.71	-2394046.90	383.92	-2393662.98
RDX+Mg	-2881624.65	370.92	-2881253.73	-2880812.37	379.81	-2880432.56
RDX+Ca	-4135749.63	358.30	-4135391.33	-4134977.86	366.84	-4134611.02
Energies in kJ/mol.						

<RDX+Ca< RDX+Be< RDX+Mg obtained by methods I and II, respectively. Whereas, the LUMO energy order follows the sequence of RDX+Mg<RDX+Ca<RDX<RDX+Be and RDX-+Mg<RDX+Ca <RDX+Be< RDX by I and II calculation methods, respectively. Consequently, the Δε values follow the order of RDX+Mg< RDX+Be< RDX+Ca <RDX in each case of the calculations. It is to be noted that the metals considered raises up the HOMO energy level as compared to RDX molecule but with the exception of Mg they do not have any great influence on the LUMO energy of RDX. Whereas, the presence of Mg lowers the LUMO energy of RDX (Figures 6,7) and (Table 3). The calcium composite system has a destroyed RDX ring thus it is completely different than the others. However, when the Be and Mg cases are compared, Mg atom somewhat lowers both the HOMO and LUMO energy levels at the level of B3LYP/6-31++G(d,p) but raises the HOMO and lowers the LUMO in the case of ω B97X-D/6-31++G(d,p). Note that presence of Mg also lowers the LUMO energy of RDX as well. The energy lowering could be attributed to donation of some electron population to RDX molecule thus it gets positive charge. On the other hand, the HOMO of the composite system spreads over the Mg atom in contrast to Be composite case (Figure 8). So, some complexation with Mg atom and RDX is expected (like complex formation of Mg and etheric oxygen atom in the Grignard reagent [30], in addition to electrostatic charge-charge interactions prevailing between the positively charged Mg atom and nearby NO2 oxygen atoms of RDX molecule.

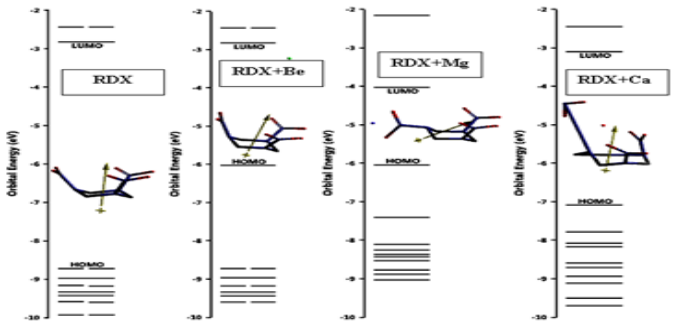

Figure 6: Some molecular orbital energies of RDX and the composites considered (B3LYP/6-31++G(d,p) level of calculations).

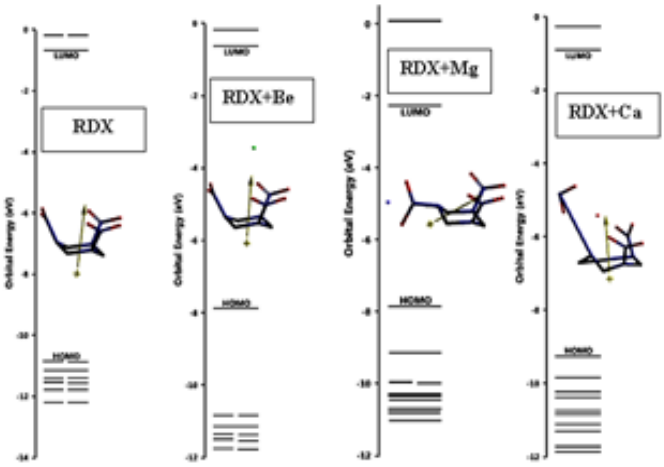

Figure 7: Molecular orbital spectra of RDX and the composites considered (ω B97X-D/6-31++G(d,p) level of calculations).

As seen in (**Figure 8**) the LUMO of RDX+Be composite system is completely confined to RDX skeleton. In the case of RDX+Mg system the HOMO and LUMO reside over the Mg atom and part of RDX structure nearby the metal atom. The HOMO of RDX+Ca system, in large part, resides over the expelled NO_2 moiety whereas it contributes nothing to LUMO of the organic moiety (the decomposed RDX skeleton). Both of the calculation methods yield similar results as depicted in the **(figure 8).**

Note that the impact sensitivity is generally correlated with the HOMO-LUMO energy gap [31]. Smaller the gap, explosive material is more sensitive to impact. Hence, the RDX+Mg composite, having much narrow interfrontier molecular orbital energy gap (Δε) should be more sensitive to impact stimulus as compared to RDX+Be composite and they are more sensitive than RDX. Although, be seems to be less activating that Mg it is highly poisonous to be used widely [32].

(Figure 9) shows the electrostatic potential maps of the composites. In the cases of Be and Mg composites, around the NO2 groups and upper part of the RDX structure are characterized with negative potential whereas the lower part of RDX skeleton possesses positive potential. In the case of RDX+Ca case the negative potential region coincides with the expelled NO2 group and partly but in lesser degree, over the remaining NO2 groups. Positive potential region covers the RDX skeleton**.**

Table 3 .The frontier molecular orbital energies and interfrontier molecular orbital energy gaps (Δε) of RDX and the composites considered.						
	B3LYP/6-31++G(d,p)			ω B97X-D/6-31++G(d,p)		
Composite	HOMO	LUMO	Δε	HOMO	LUMO	Δε
RDX	-841.26	-271.90	569.36	-1047.69	-64.44	983.25
RDX+Be	-581.71	-272.68	309.03	-760.45	-61.27	699.18
RDX+Mg	-582.67	-388.29	194.38	-758.12	-218.85	539.27
RDX+Ca	-683.74	-298.93	384.81	-892.65	-87.14	805.51
Energies in kJ/mol.						

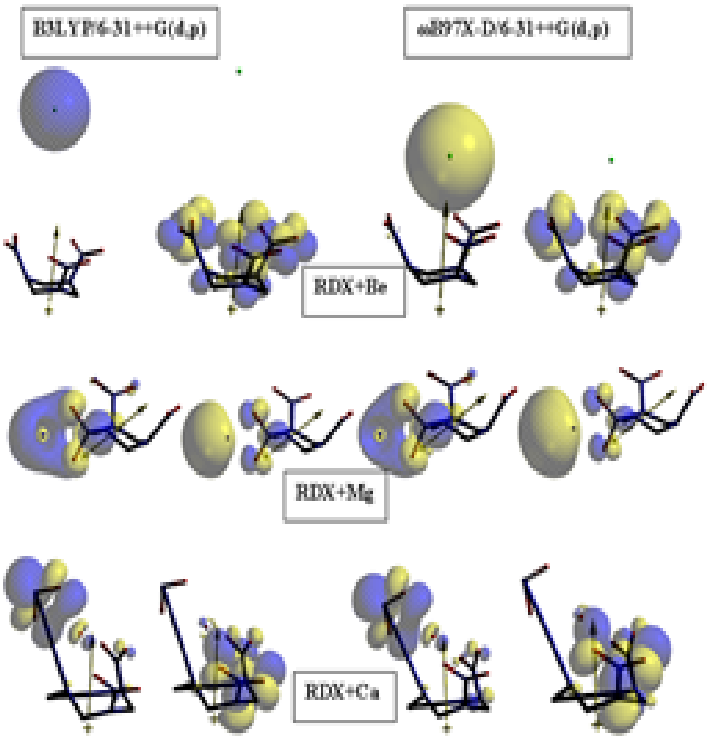

Figure 8: The HOMO and LUMO pattern of the composites.

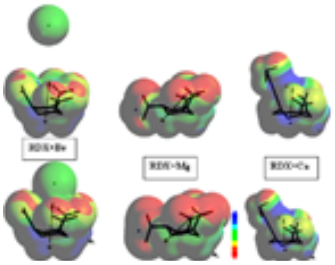

Figure 9: Electrostatic potential maps of the composites (upper and lower rows stand for B3LYP/6-31++G(d,p) and ω B97X-D/6-31++G(d,p) level of calculations, respectively).

Conclusion

The present calculations indicate that Be and Mg atoms do not cause any drastic effect on RDX molecule so in their composites RDX ring system remains intact. However, calcium atom dramatically affects RDX molecule by causing the ring rupture and expelling one of the nitro groups. In every case, metal atom acquires some positive charge, which is indicative of transfer of some electron population to highly electron demanding RDX molecule. The expelled NO_2 moiety is in the form of pre-nitrite. Each metal atom highly affects the energies of the HOMO and LUMO levels. The presence of metals considered narrows the inter frontier molecular orbital energy gap of RDX suggesting that the corresponding composites are more sensitive to impact than RDX is. In that sense, Mg is more effective.

References

1. Akhavan J: The Chemistry of Explosives. UK: The Royal Society of Chemistry; 2004.

2. Agrawal JP: High Energy Materials, Propellants, Explosives and Pyrotechnics.Weinheim: Wiley-VCH; 2010.

3. Agrawal JP, Hodgson, R. D.: Organic Chemistry of Explosives. Sussex: Wiley; 2007.

4. Fordham S: High Explosives and Propellants. Oxford: Pergamon;1980.

5. Ledgard JB: The preparatory Manual of Explosives. USA: 2007.

6. Zhu W, Xiao J, Zhu W. et al. Molecular dynamics simulations of RDX and RDX–based plastic–bonded explosives. J Hazard Mater 2009;164(2-3):1082–1088.

7. Keshavarz HM.Simple relationship for predicting impact sensitivity of nitroaromatics,nitramines,and nitroaliphatics. Propellants, Explosives, Pyrotechnics 2010; 35:175–181.

8. Sikder AK, Maddala G, Agrawal JP. et al. Important aspects of behavior of organic energetic compounds: A review. J Hazardous Mater; 2001; A84: 1–26.

9. Mader CL.Numerical Modeling of Explosives and Propellants. New York: CRC Press:1998.

10. Köhler J, Meyer R, Homburg A.: Explosives. Weinheim: VCH; 1993.

11. Scott MA, Petrova T, Hill F.et al. Density functional theory study of interactions of cyclotrimethylene trinitramine (RDX) and triacetone triperoxide (TATP) with metal-organic framework (IRMOF-1(Be)). Structural Chemistry. 2012,23(4): 1143-1154.

12. Ausherman DR, McKinnon CN Jr. Detonation hydrodynamics for condensed explosive with inert additives. Astronautica Acta. 1970;15(5-6):439-52.

13. Weiser V, Kelzenberg S, Knapp S.et.al. Methods to investigate the igniter /propellant interaction**,** International Annual Conference of ICT 43rd (Energetic Materials) 2012 ;69/1-69/10.

14. De Paz JLG,Ciller J. On the use of AM1 and PM3 methods on energetic compounds.Propellants, Explosives, Pyrotechnics 1993; 18: 33-40.

15. Osmont A, Catoire L, Gökalp I.et al.Ab initio quantum chemical predictions of enthalpies of formation, heat capacities, and entropies of gas–phase energetic compounds. Combustion and Flame. 2007; 151:262–273.

16. Mocella C,Conkling JA: Chemistry of Pyrotechnics. Boca Raton: CRC press;1985.

17. Stewart JJP. Optimization of parameters for semiempirical methods I. Method. J Comput Chem 1989;10: 209-220.

18.Stewart JJP. Optimization of parameters for semi empirical methods II. Application. J Comput Chem1989;10: 221-264.

19. Leach AR: Molecular Modeling. Essex :Longman;1997.

20.Fletcher P: Practical Methods of Optimization. New York :Wiley;1990.

21. Kohn W, Sham L. Self-consistent equations including exchange and correlation effects. J Phys Rev 1965;140:1133-1138.

22. Parr RG, Yang W: Density Functional Theory of Atoms and Molecules. London: Oxford University Press;1989.

23. Minenkov Y, Singstad A, Occhipinti G, Jensen VR. The accuracy of DFT-optimized geometries of functional transition metal compounds: a validation study of catalysts for olefin metathesis and other reactions in the homogeneous phase. Dalton Trans. 2012,41(18):5526-41.

24.Kozuch S, Martin JML, Halogen bonds: Benchmarks and theoretical analysis. J.Chem. Theory Comput. 2013;9: 1918–1931.

25. Becke AD, Density-functional exchange-energy approximation with correct asymptotic behavior. Phys Rev A. 1988, 38: 3098-3100.

26.Vosko H S, Wilk L, Nusair M. Accurate spin-dependent electron liquid correlation energies for local spin density calculations: a critical analysis.Can J Phys 1980; 58:1200-1211.

27. Lee C, Yang W, Parr RG. Development of the Colle-Salvetti correlation-energy formula into a functional of the electron density. Phys Rev B 1988; 37: 785-789.

28. SPARTAN 06, Wavefunction Inc, Irvine CA, USA; 2006.

29. Durant PJ, Durant B: Introduction to Advanced Inorgan-

ic Chemistry. London:Longman; 1970.
30. Nesmeyanov AN, Nesmeyanov NA: Fundamentals of Organic Chemistry. Moscow:Mir;1981.
31.Badders RN, Wei C, Aldeep AA.et.al. Predicting the impact sensitivity of polynitro compounds using quantum chemical descriptors. J. of Energetic materials. 2006; 24: 17-33.
32. Dreisbach RH. Handbook of Poisoning. Los Altos, California: Lange Medical Pub,1971.